Short time Fourier transform analysis for understanding frequency dependent attenuation in austenitic stainless steel

Article *in* NDT & E International · January 2013

DOI: 10.1016/j.ndteint.2012.09.001.

CITATIONS
34

READS
177

5 authors, including:

Govind K. Sharma
Indira Gandhi Centre for Atomic Research
26 PUBLICATIONS **188** CITATIONS

SEE PROFILE

Anish Kumar
Indira Gandhi Centre for Atomic Research
169 PUBLICATIONS **1,787** CITATIONS

SEE PROFILE

Babu Rao Dr C
Indira Gandhi Centre for Atomic Research
102 PUBLICATIONS **554** CITATIONS

SEE PROFILE

Baldev Raj
Indira Gandhi Centre for Atomic Research
919 PUBLICATIONS **18,386** CITATIONS

SEE PROFILE

NDT&E International 53 (2013) 1–7

Contents lists available at SciVerse ScienceDirect

NDT&E International

journal homepage: www.elsevier.com/locate/ndteint

Short time Fourier transform analysis for understanding frequency dependent attenuation in austenitic stainless steel

Govind K. Sharma, Anish Kumar*, C. Babu Rao, T. Jayakumar, Baldev Raj

Metallurgy and Materials Group, Indira Gandhi Centre for Atomic Research, Kalpakkam 603102, Tamil Nadu, India

ARTICLE INFO

Article history:
Received 22 July 2011
Received in revised form
11 July 2012
Accepted 7 September 2012
Available online 24 September 2012

Keywords:
Ultrasonic scattering
Grain size
Short time Fourier transform (STFT)
Austenitic stainless steel

ABSTRACT

Short time Fourier transform (STFT) has been used to study the distribution of ultrasonic energy as a function of the frequency of the wave in the backscatter and the back-wall echoes obtained from austenitic stainless steel specimens with different grain sizes in a range of 30–210 μm. A 25 MHz nominal frequency immersion transducer was used in pulse-echo mode for data acquisition. In specimens with larger grain sizes (> 100 μm), the frequency content of the first back-wall echo was 4.5–7.0 MHz only whereas the predominant frequency of the backscatter was in a range of 15–25 MHz up to the third/fourth back-wall echo. The amplitude and the frequency content of the back-wall echoes decreased rapidly with the propagation distance, however those of the backscatter decreased very slowly indicating high scattering and low absorption rates in the austenitic stainless steel specimens. The decrease in the center frequency of the first, second and third back-wall echoes has been correlated with the average grain size. The study demonstrates the usefulness of STFT in analyzing the frequency content of the backscatter and back-wall echoes simultaneously and thus understanding the frequency dependent attenuation in high scattering materials for microstructural characterization applications.

1. Introduction

Ultrasonic wave traveling through solids is subjected to scattering and mode conversion as the wave advances through the material and encounters the grain boundaries. The received ultrasonic signal is a non-explicit function of the average grain diameter, ultrasonic wavelength, inherent anisotropic character of individual grains and random orientation of crystallites. Therefore, it has been possible to estimate the average grain size by analyzing the received ultrasonic signal [1]. The propagation of an ultrasonic wave in an anisotropic material depends on the frequency of the ultrasonic waves. The attenuation experienced at higher frequencies is generally larger than at lower frequencies. An ultrasonic wave propagating through such a medium will suffer spectral distortion due to high rate of attenuation of its high frequency components. This results in a change in the center frequency of its power spectrum [2,3]. Ultrasonic spectral analysis was used in both nondestructive testing [2–7] and medical imaging [8–10]. Often in testing materials nondestructively, spectral analysis is used for characterizing the microstructure, flaw detection and sizing [4–7]; whereas, in medical imaging, spectral analysis of scattered echoes had been useful in characterizing the tissues [8–10].

Fourier transform based methods have been applied to estimate the effect of grain size on frequency dependent attenuation [2,3]. The spectral shifts were correlated with grain size of anisotropic materials such as stainless steel [2,3,11]. Special signal processing methods such as homomorphic processing has been applied for characterization of backscattered grain noise. The homomorphic processing is capable of smoothening the power spectrum of backscatter signal, and can be used for estimating the frequency shift resulting from grain scattering [11,12]. The homomorphic processing operations are done with backscatter signals, however, only Fourier methods are applied to evaluate frequency content of the back-surface echo. The estimation of back-surface echo frequency using Fourier transform is valid when the analysis is done on the signal with good signal to noise ratio (SNR). As the grain size increases, SNR decreases due to higher grain scattering, and the back-wall echo frequency shifts toward lower side but the frequency content of the backscatter noise may still be higher [11,12]. This can cause serious errors in estimating frequency content at the region of interest in the ultrasonic signal e.g. for a back-wall echo. The complete understanding of such system (frequency dependent attenuation) can be enhanced by using Joint time frequency analysis (JTFA) methods due to non-stationary nature of the signal [13–15]. JTFA methods can provide comprehensive information about the signal features simultaneously in both time and frequency domain

* Corresponding author.
E-mail address: anish@igcar.gov.in (A. Kumar).

0963-8695/$ - see front matter © 2012 Elsevier Ltd. All rights reserved.
http://dx.doi.org/10.1016/j.ndteint.2012.09.001

and hence can provide in depth understanding of such a system. Time frequency analysis has been used primarily to enhance the sensibility of flaw detection, to measure thin materials thickness and to characterize defects in nature (planar or volumetric) [16]. It has also been used for the determination of phase velocity in the plexiglass material [14]. Recently, STFT has been used for the material property characterization regarding the individual effects of steel bar corrosion in concrete, hydration and moisture content distribution of construction materials [17].

The short-time Fourier transform (STFT) is one of the earliest and the most basic method used for time-frequency analysis. Another commonly used time-frequency distribution (TFD) methodology is the Wigner–Ville distribution (WVD). Theoretically, the WVD has an infinite resolution in time due to absence of averaging over any finite time interval. Moreover for infinite lag length, it has an infinite frequency resolution. The WVD being quadratic in nature introduces cross terms for a multicomponent signal. The cross terms can have significant amplitudes and they can corrupt the transform space [18–20]. The Wigner distribution gives better auto term localization compared to the smeared out STFT. However, when applied to a signal with multi frequency components the presence of cross terms may lead to an ambiguous analysis. Hence, in the present study we have used STFT for determination of spectral contents of backscatter and back-wall echoes.

The STFT is one of the most widely used algorithms in JTFA based on detail Fourier transform centered at each time point. In STFT, the signal is compared with window functions that are concentrated in both time and frequency domains. The spectra at any particular time are then stacked to reflect the lateral variation of signal behavior in both time and frequency in JFTA. The STFT algorithm and the window function can be mathematically represented as Eq. (1):

$$\mathrm{STFT}[s(t)] = S(\tau,\omega) = \int_{-\infty}^{+\infty} s(t)\chi(t-\tau)e^{-j\omega t}dt \quad (1)$$

where, $\chi(t)$ is the window function which has a user defined time duration; and $s(t)$ is the waveform signal in time domain. This operation (Eq. 1) differs from the Fourier transform only by the presence of window function $\chi(t)$. As the name implies, the STFT is generated by taking the Fourier transform of smaller durations of the original waveform. Alternatively, we can interpret the STFT as the projection of the function $s(t)$ onto a set of bases $\chi(t-\tau)e^{-j\omega t}$ with parameters t and ω. Since the bases are no longer of infinite extent in time, it is possible to monitor how the signal frequency spectrum varies as a function of time. This is accomplished by the translation of the window as a function of time t, resulting in a 2D joint time–frequency representation STFT(t,ω) of the original time signal. The magnitude display $|\mathrm{STFT}\ (t,\omega)|^2$ is called the spectrogram of the signal. The result of analysis depends on the choice of the window function leading to a trade off between time localization and frequency resolution. If the window length is too small, spectral leakage of low frequency component appear and when it is too long, the target of interest would be blurred [21].

In one of our previous studies [2,3] the peak frequency in the autopower spectrum of the first back-wall echo was linearly correlated with inverse of the square root of grain size in an austenitic stainless steel. This methodology for grain size measurement has special practical advantage due to its independence on the coupling conditions and requirement of only one back-wall echo [3]. Even though the peak frequency could be correlated with the grain size effectively for smaller grain sizes, unambiguous determination of the peak frequency could not be possible in specimens with larger grain sizes (>140 μm) due to the poor SNR.

A signal processed with the classical Fourier transform illustrates the frequency distribution over the entire signal window. It is compared to sinusoidal functions that spread over the entire signal and are not connected in any particular ultrasonic pulse timings. As a result, the classical Fourier transform does not explicitly evaluate the evolution of frequency contents with time in non-stationary signal such as in high ultrasonic scattering materials. In the present study, STFT based JTFA is adopted to understand the frequency dependent attenuation in 316 stainless steel, a high scattering material. It is also explored if the limit of the spectral analysis based approach for grain size measurement can be extended for larger grain size specimens by using STFT analysis. This has a beneficial implication on the potential for inspection of coarser grain and higher thickness materials for defect detection with higher sensitivity.

2. Experimental

Several specimens of AISI type 316 stainless steel (50 mm diameter and 12 mm thickness) were obtained from bar stock. The chemical composition of the material used is as follows: C-0.06, Mn-1.80, Si-1.00, Cr-16.36, Ni-12.1, Mo-2.2 and Fe- balance. The specimens were heat treated at different temperatures varying from 1373 K to 1623 K for different time durations (15–180 min) in order to obtain the specimens with varied grain sizes. Subsequently, all the specimens were given a common treatment at 1323 K for 30 min followed by water quench in order to obtain a uniform structure with same substructural features except for the variations in the grain size [22]. Specimens of size 40 mm × 30 mm with 10 mm thickness were prepared from these heat treated samples. Subsequently, surface grinding of the specimens was

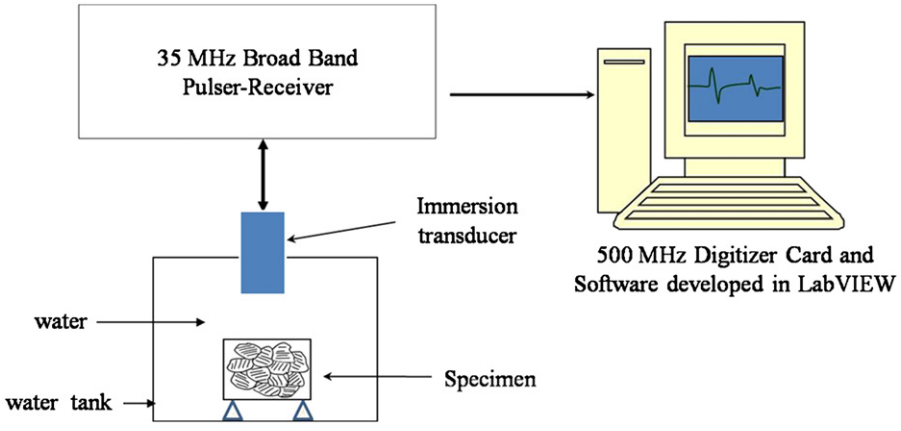

Fig. 1. Schematic of the experimental set-up for ultrasonic measurements.

carried out to obtain plane parallelism to an accuracy of better than 3 μm. Metallographic examinations were carried out to reveal the grain structure in different specimens. The linear intercept method as per ASTM standard E112-96 [23] was used to measure the average grain size for correlation with the ultrasonic parameters.

The experimental setup used for the ultrasonic immersion measurements is shown in Fig. 1. A 6 mm diameter, 25 MHz unfocused (16 MHz center frequency), immersion transducer (supplied by M/s. Panametrics, USA) and 35 MHz broadband ultrasonic pulser receiver (M/s. Panametrics, USA) were used. The gated waveforms of 15 μs length, including the water specimen reflection and time scale corresponding to three back-wall echoes, were digitized at 500 MS/s using a digitizer (M/s. Acquiris, 500 MHz) and were stored in ASCII format using a LabVIEW program. All the waveforms were averaged for 100 times to eliminate random noise from electronic equipments. The specimens were kept in the far field of the transducer. The center frequency of the transducer is measured as the peak frequency in the front surface reflection keeping it at 80% of full scale height (FSH). Back-wall echo frequency was determined by keeping the first back wall (FBW) height to 80% of FSH.

The optimization of window length is crucial for STFT as it governs the resolutions in both time and frequency. As the window length decreases, the time resolution increases and the frequency resolution in STFT decreases. The frequency resolution can be maintained by zero padding, however, a shorter window length leads to spectral leakage. A methodology has been devised to determine the optimum window length automatically. The top surface echo of specimen P0, for which the central frequency and −3 dB bandwidth were measured to be 15.9 MHz and 4.1 MHz, respectively by FFT, was chosen for the standardization of the window length. An algorithm was developed in LabVIEW for transforming A-scan signals to 2D time–frequency plots (spectrogram) and to measure the peak frequency and the −3 dB bandwidth at the back-wall echo locations automatically. The window length was increased in a step of 0.128 μs (64 data points) and the peak frequency corresponding to the maximum in time domain and −3 dB bandwidth for each window length were determined automatically by STFT, after making the total window length to 4.096 μs (2048 data points) by suitable zero padding.

Fig. 2 shows the variations in the peak frequency and the −3 dB bandwidth with the data length. It can be seen in Fig. 2 that with increase in the window size from 0.2 to 2.5 μs, the peak frequency decreases from 16.8 MHz to 15.8 MHz and the −3 dB bandwidth decreases from 5.8 MHz to 4.2 MHz. For the window lengths of more than 1.024 μs (512 data points), the peak frequencies and the −3 dB bandwidth obtained from STFT are comparable to those obtained from the FFT of the selected echo (Fig. 2). Hence, a window length of 1.024 μs has been selected for STFT analysis in the present study. This is an objective measure independent of manual selection of the time window, which alleviates and reconciles the trade-offs regarding the spectral leakage (due to too small time window), and unclear target of interest (due to too large time window) in STFT spectrogram. The A-scan (one dimensional) signals corresponding to different grain size specimens were normalized with respect to the peak amplitudes of the first back-wall signal and windowed with a continuously moving Hamming window of 1.024 μs (512 discrete data points) length. The maximum and minimum frequency corresponding to backscatter is calculated by analyzing the spectrograms. Average of five readings for the peak frequency is given for each specimen. The maximum scatter in the measurement of peak frequency was ±0.20 MHz for all the specimens at the region of interest.

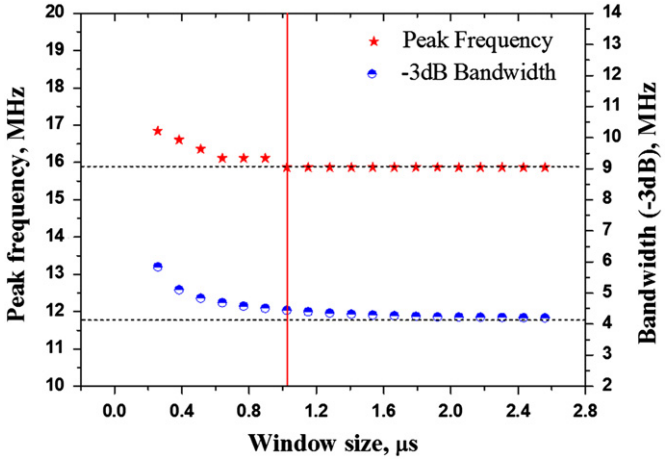

Fig. 2. Effect of the time window size for generating spectrogram on the measured peak frequency and −3 dB bandwidth. Dotted lines show peak frequency and −3 dB bandwidth obtained by FFT. (The results are shown for the top surface echo of the specimen with 30 μm grain size, for which the center frequency and −3 dB bandwidth were measured to be 15.9 MHz and 4.13 MHz, respectively.)

3. Results

Table 1 provides the details of the heat treatments given to the samples. Typical micrographs showing the variations in the grain size with different heat treatment conditions are shown in Fig. 3 and the corresponding average grain sizes obtained are given in Table 1. Fig. 4(a) shows a typical rf ultrasonic signal and its spectrogram obtained for a specimen with an intermediate grain size (121 μm). The backscatter amplitude during the water path (before the front surface reflection) is negligible. However, as the beam enters into the material, a sudden increase in the backscatter amplitude can be observed clearly after the water–specimen interface echo. Fig. 5 shows change in the frequency content of the first three back-wall echoes for the intermediate grain size (121 μm) specimen. The amplitude of the back-wall echoes decreased and the spectrum shifted marginally towards lower frequency with increasing propagation distance.

The spectrogram show that the frequency content of the backscatter noise is in a range of 14–24 MHz for all the specimens (Figs. 4, 6 and 7). However, the peak frequency of the first back-wall echo is much lower as compared to the peak frequency of the front surface reflection (~16 MHz) and decreases with increasing grain size (Figs. 6 and 7). With increasing grain size, the amplitude of the backscatter increased and the amplitude of the back-wall echoes decreased (Figs. 6 and 7). The frequency content of the backscatter signal obtained even after the first and the second back-wall echoes is much higher than that of the first back-wall echo.

The effect of grain size on the peak frequencies of the first three back-wall echoes, as obtained from the spectrogram, are shown in Fig. 8 and Table 1. As multiple peaks were observed in the spectra of the backscatter, providing a single peak frequency would be misleading, hence a range of frequency is shown for the frequency content of the backscatter signal.

4. Discussion

The observed effect of the grain size on the frequency content of the back-wall echoes and the backscatter signal can be explained on the basis of the ultrasonic scattering theory. The scattering and absorption are responsible for change in the spectral parameters of ultrasonic signal. The total attenuation co-efficient α may be expressed as $\alpha=\alpha_a+\alpha_s$, where α_a stands for the losses due to internal friction, i.e. ultrasonic absorption, and α_s takes into account losses due to the scattering of the ultrasonic waves. Ultrasonic absorption consists of the thermoelastic losses,

Table 1
Details of the heat treatments given to AISI Type 316 stainless steel specimens, corresponding average grain sizes and the peak frequencies in the front surface (FS) echo, first back-wall echo (FBW), second-wall echo (FBW) and third back-wall echo (TBW).

Specimen ref. no.	Heat treatment	Grain size (μm)*	Peak frequency, FS (MHz)	Peak frequency, FBW (MHz)	Peak frequency, SBW (MHz)	Peak frequency, TBW (MHz)
P0	As received	30	15.6	15.2	14.8	14.7
P1	1373 K/1 h/WQ	63	15.9	8.56	7.88	7.23
P2	1373 K/1.25 h/WQ	78	16.1	8.33	7.61	6.9
P3	1573 K/1.5 h/WQ	106	16.1	7.08	6.23	5.71
P4	1623 K/0.5 h/WQ	121	15.6	6.51	5.45	4.61
P5	1623 K/1 h/WQ	138	16.1	6.12	4.93	4.59
P6	1623 K/3 h/WQ	210	16.1	4.46	3.63	–

Note: WQ—Water Quench.

* From optical metallography (ASTM standard E12-88).

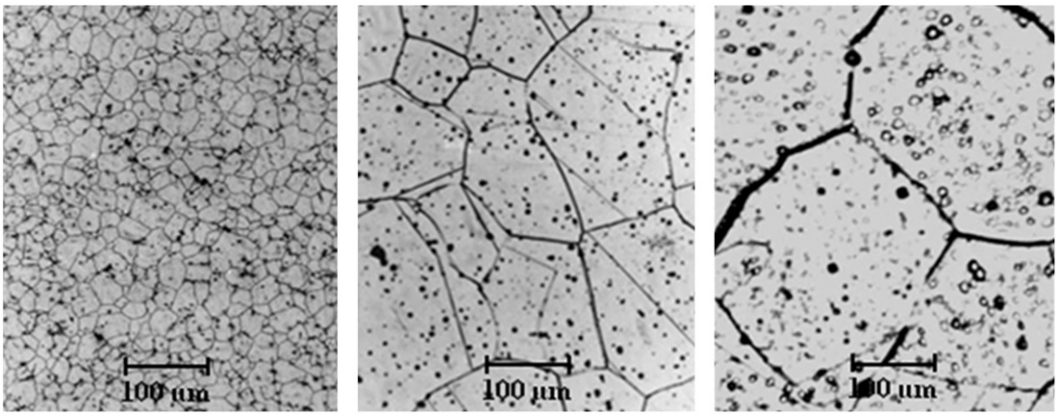

Fig. 3. Photomicrographs of the stainless steel specimens with (a) 30 μm, (b) 78 μm and (c) 210 μm grain size.

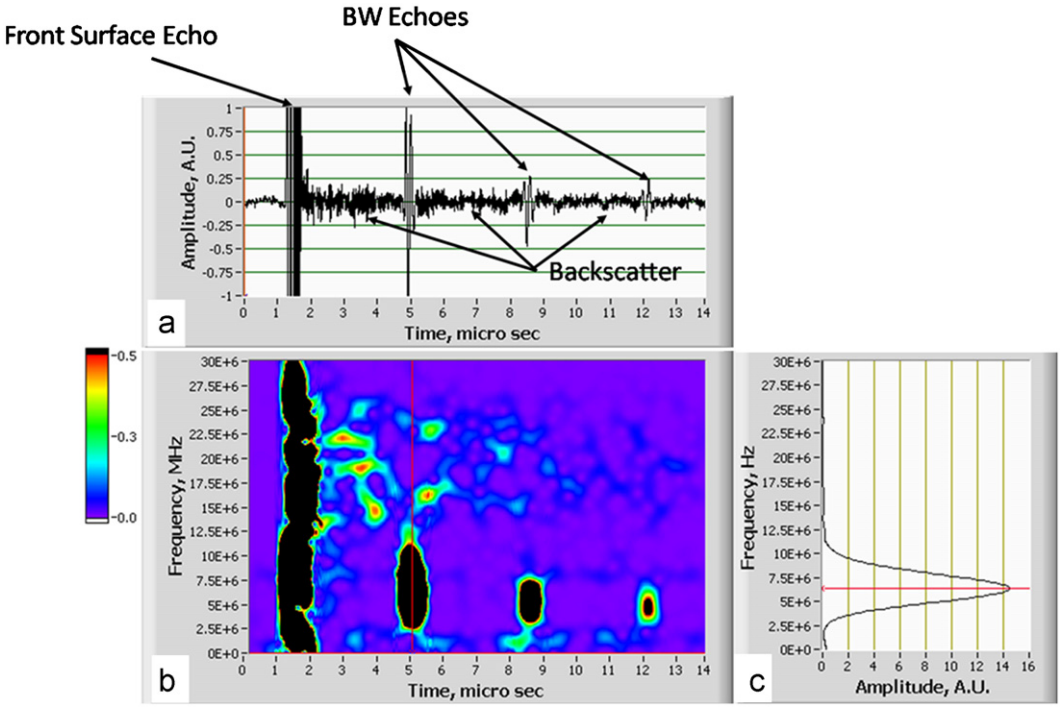

Fig. 4. (a) Time domain signal from specimen of 121 μm grain size specimen and (b) its specgram (c) frequency content of first back-wall.

magnetic losses and losses due to dislocation damping. For a non-ferromagnetic material, like austenitic stainless steel, absorption is due to the thermoelastic losses and losses due to dislocation damping only. The absorption co-efficient α_a can be expressed as [24], $\alpha_a = a_1 f^{0.5} + a_2 f^2$, where a_1 and a_2 are the constants and f is the frequency. The first and second terms in right hand side of the equation take into account the thermoelastic losses and losses due to dislocation damping respectively.

The scattering in polycrystalline materials is dominated by Rayleigh scattering when the wavelength of the ultrasonic waves (λ) is greater than the grain size (d). In the present study, the ratio of grain size to wavelength lies in a range of 0.08–0.55 ($V=5750$ m/s, $\lambda=360$ μm for 16 MHz center frequency and values of d are from 30 to 210 μm, indicating Rayleigh scattering is predominant. The ultrasonic scattering coefficient due to the Rayleigh scattering (α_s) in polycrystalline materials [25,26] can be expressed as

$$\alpha_s = Sd^3f^4 \tag{2}$$

where S is a scattering factor that depends on the elastic anisotropy of the crystallites, d is the average grain size in the specimen and f is the frequency.

At the water–steel interface, a high frequency ultrasonic beam (~16 MHz center frequency) enters into the material. As scattering is a function of the fourth power of the frequency (Eq. (2)), the higher frequency components of the signal get preferentially scattered in all directions. The high frequency backscattered energy is received by the transducer and comparatively lower frequency beam continues to propagate deeper into the material and return to the transducer as a low frequency back-wall echo. This explains the higher frequency content of the backscatter and lower frequency content in the back-wall echo. The high frequency scattered energy keeps returning to the transducer due to multiple scattering and reflections of the originally scattered energy from the grains and the specimen boundaries in the direction of the transducer, until they are totally lost in the material due to absorption phenomena. As the absorption phenomena are weak functions of the frequency (as compared to the Rayleigh scattering), the decrease in the frequency content of the backscatter signal is much smaller. This explains the high frequency content (15–25 MHz) of the backscatter noise even up to the time path of the third back-wall echo. Further, as all the specimens were given a similar final heat treatment, the dislocation substructure is expected to be similar, hence almost similar decay rate of the backscattered signal is observed in all the specimens [22].

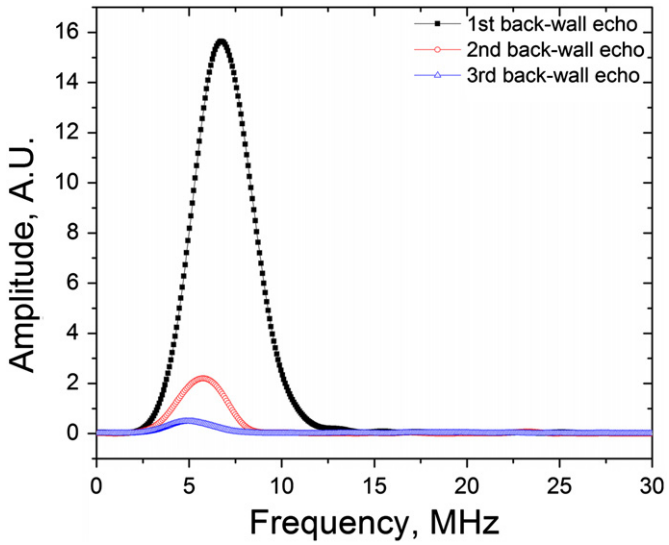

Fig. 5. The frequency content of the first three back wall echoes using STFT for 121 μm grain size specimen.

The effect of the grain size on the frequency content of the back-wall echoes can also be understood by the spectral analysis of the attenuating ultrasonic wave. It can be assumed that the oscillatory amplitude decays exponentially as the propagation length of the ultrasonic wave increases. If we consider the spectral distribution of the ultrasonic wave, which has an oscillatory pulse of one or two cycles with an exponential decay envelope, the amplitude of the ultrasonic wave $g(t)$ is expressed as

$$g(t) = Ae^{-\alpha t}\sin(2\pi f_0 t - \phi) \quad \phi/f_0 < t < 2 + \phi/f_0 \tag{3}$$

where α is the attenuation coefficient, t is time, f_0 is the carrier frequency, ϕ is phase and A is maximum amplitude of the pulse wave. The spectrum power distribution $|G(f)|^2$ is derived by Fourier transform [27]:

$$|G(f)|^2 \alpha \frac{1+\exp(-2\alpha/f_0)-2\exp(-\alpha/f_0)\cos 2\pi(f-f_0)/f_0}{\alpha^2+4\pi^2(f-f_0)^2} \tag{4}$$

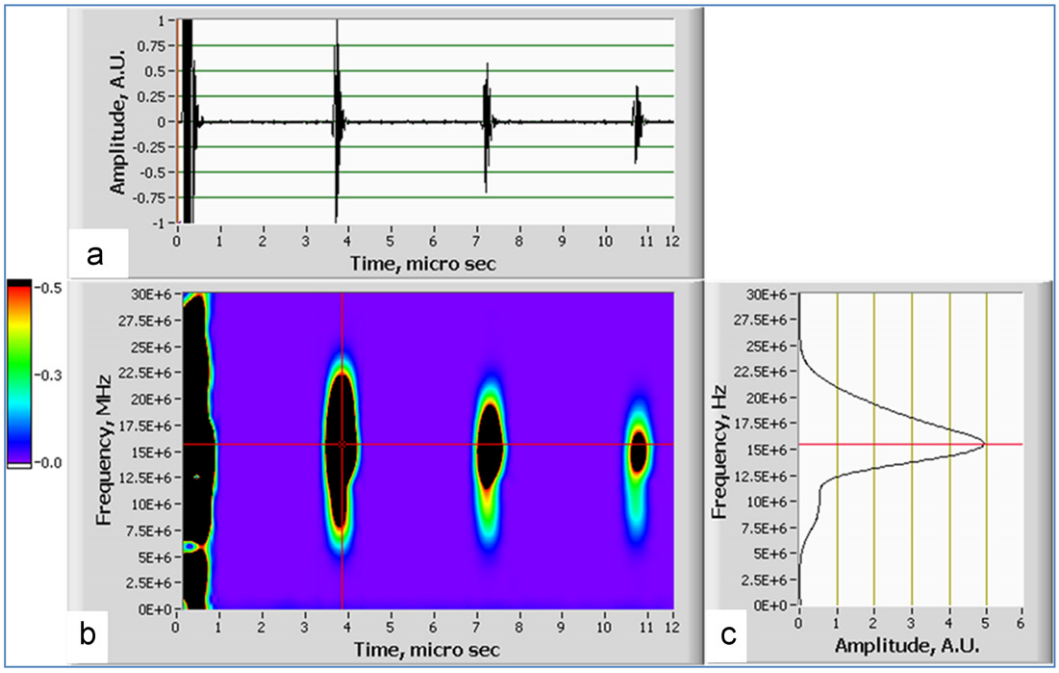

Fig. 6. (a–c) A-scan, specgram and frequency transform of the first back-wall for 30 μm grain size specimens. The location of the first back-wall echo is shown by cross of the cursors.

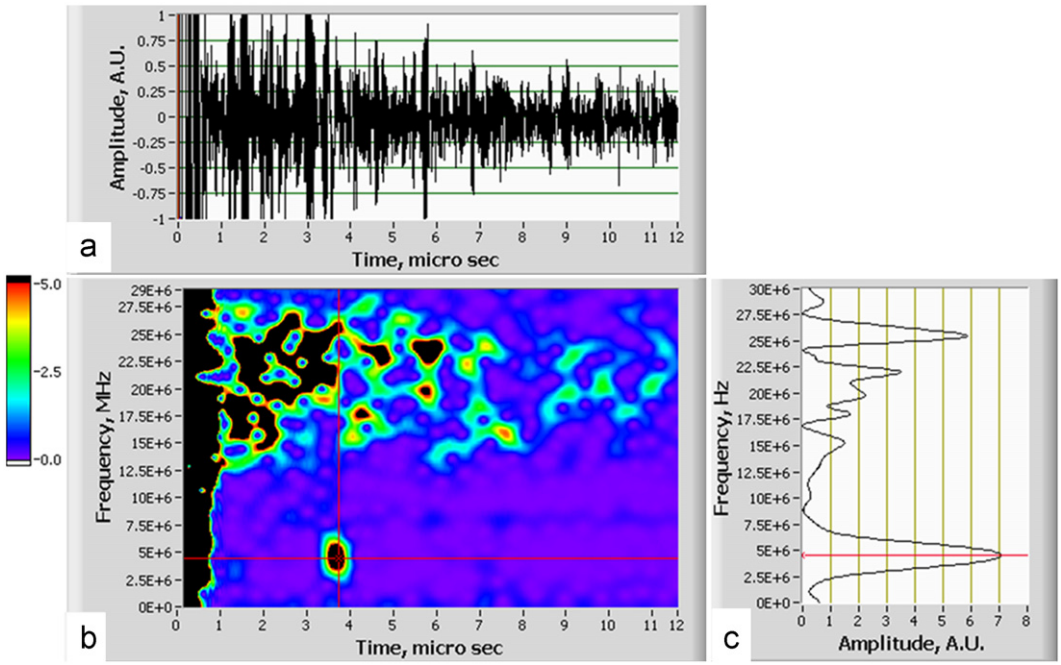

Fig. 7. (a–c). A-scan, specgram and frequency transform of the first back-wall for 210 μm grain size specimens. The location of the first back-wall echo is shown by cross of the cursors.

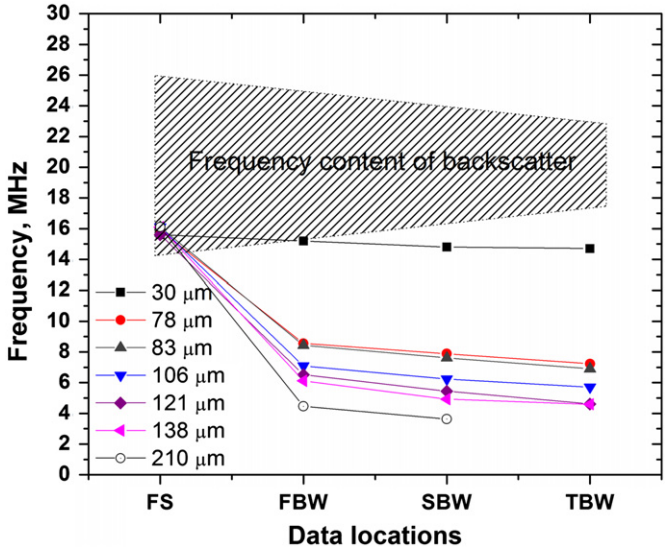

Fig. 8. Variation in the peak frequencies of front surface (FS) reflection, first (FBW), second (SBW) and third (TBW) back-wall echoes. The range of spectral content of the backscatter is also shown.

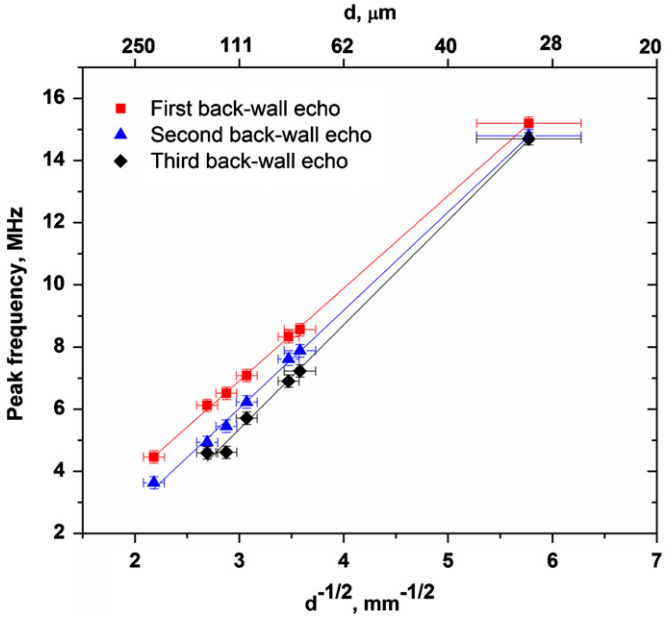

Fig. 9. Correlation between peak frequencies of first, second and third back-wall echoes with the grain size.

In an austenitic stainless steel, more than 95% of the total attenuation is caused by the scattering [28], hence α in Eq. (6) can be replaced by α_S of Eq. (4). As the grain size increases, α_S increases as a function of its third power (Eq. (4)). With increase in α_S, the peak frequency of the autopower spectrum shifts to lower values due to the fourth power dependence of α_S on frequency. Because of this, the peak frequency shifts towards lower values with increase in the grain size.

In one of our previous studies [2,3], the peak frequency in the autopower spectrum of the first back-wall echo was linearly correlated with inverse of the square root of grain size for the same specimens as investigated in the present study. The ultrasonic signals were acquired using a 25 MHz contact transducer and the peak frequency of the first back-wall echo was determined using Fourier transform. Even though the peak frequency could be correlated with the grain size effectively for smaller grain sizes, unambiguous determination of the peak frequency could not be possible in specimens with larger grain sizes (>140 μm) due to poor SNR [3]. This can be seen in Fig. 6a and c. The back-wall echo is submerged in the backscatter noise due to high scattering in the large grain size (210 μm) specimen. The back-wall echo can neither be distinguished in the time domain nor in the frequency spectrum. However, the back-wall echo with even such a poor SNR also stands out clearly in the spectrogram (Fig. 7b). Using spectrogram, it can be clearly understood that the lower frequency peak in the frequency spectrum (Fig. 7c) is from the back-wall echo, while the higher frequency peaks are from backscatter noise. This demonstrates the

advantage of the JTFA based approach over conventional frequency spectrum based analysis for microstructural characterization applications.

The peak frequency of the second and the third back-wall echoes could also be determined unambiguously using STFT analysis. The variations in the peak frequency of the first three back-wall echoes exhibited linear relationships with $d^{-1/2}$ as follows (Fig. 9):

$$PF_{FBW} = -2.0 + 2.89d^{-1/2} (R = 0.97) \quad (5)$$

$$PF_{SBW} = -3.7 + 3.14d^{-1/2} (R = 0.97) \quad (6)$$

$$PF_{TBW} = -5.3 + 3.39d^{-1/2} (R = 0.96) \quad (7)$$

where, PF_{FBW}, PF_{SBW}, and PF_{TBW} are the peak frequencies in the first, second and third back-wall echoes respectively, and d is the average grain size measured by optical microscopy. The slope of the above correlation increases from the first to the third back-wall echo continuously, indicating that the sensitivity of the spectral peak frequency based methodology for grain size measurement improves with increasing wave–material interaction distance.

The present study reports a systematic study on the application of STFT for studying frequency dependent attenuation in specimens with different extent of scattering i.e. stainless steel specimens with different grain sizes. Even though, the time-frequency analysis has been a popular choice for many authors in the area of flaw characterization or signal to noise ratio (SNR) enhancements in high scattering materials, to the best of our knowledge, the present study is a first of its kind attempt for materials characterization using time frequency analysis. The simultaneous spectral content information of the back-wall and the backscatter signals is available in a spectrogram. This provides clear visualization of the distribution of the input frequency in the backscatter and back wall echoes. This has been effectively utilized to analyze the absorption and the scattering phenomenon simultaneously. Further, the time frequency analysis could also extract back-wall echoes from noisy ultrasonic signals without any ambiguity. Using the STFT analysis, it was also possible to extend the limit of the grain size measurement using the spectral analysis approach. Further, a detailed methodology for optimization of window length for STFT has also been devised in the present study. Even though the present study is confined to the effect of the grain size, the analysis described in the present study will be equally useful for defect detection and characterization in highly attenuating thick materials.

5. Conclusions

The short term Fourier transform (STFT) time–frequency analysis is established as a useful tool for material characterization applications. It has led to a better understanding of the distribution of spectral content in an ultrasonic signal obtained from high scattering material i.e. austenitic stainless steels. The STFT analysis also helps in understanding the contribution of the scattering and the absorption to the total attenuation. The present study demonstrates that the STFT analysis can be used to effectively bring out the reflections submerged in the backscatter noise. Hence, it is easy to estimate the frequency content of the back-wall echoes and it eliminates the uncertainty in the frequency estimation in highly scattering and thick materials. The limits on the attenuation measurements on large grain size stainless steel material can be extended by using the discussed methodology. This methodology will be further extended for detection and characterization of defects in stainless steel weldments.

References

[1] Bilgutay NM, Li X, Saniie J. Spectral analysis of randomly distributed scatterers for ultrasonic grain size estimation. Ultrasonics 1989;27:19–25.
[2] Kumar Anish, Jayakumar T, Palanichamy P, Raj Baldev. Influence of grain size on ultrasonic spectral parameters in AISI type 316 stainless steel. Scripta Mater 1999;40(3):333–40.
[3] Kumar Anish, Jayakumar T, Raj Baldev. Ultrasonic spectral analysis for microstructural characterization of austenitic and ferritic steels. Philos Mag 2000;A 80:2469–87.
[4] Bouda Badidi, Lebaili S, Benchaala A. Grain size influence on ultrasonic velocities and attenuation. NDT&E Int 2003;36:1–5.
[5] Bilgutay NM, Saniie J. The effect of grain size on flaw visibility enhancement using split spectrum processing. Mater Eval 1984;42:808–14.
[6] Willems H, Goebbels K. Characterization of microstructure by backscattered ultrasonic waves. Met Sci 1981;15:549–54.
[7] Hecht A, Thiel R, Neumann E, Mundry E. Nondestructive determination of grain size in austenitic stainless sheet by ultrasonic backscattering. Mater Eval 1981;39:934–8.
[8] Chivers RC, Hill CR. Ultrasonic attenuation in human tissue. Ultrasound Med Biol 1975;2:25–9.
[9] Narayana PA, Ophir J. Spectral shifts of ultrasonic propagation: a study of theoretical and experimental studies. Ultrason Imaging 1983;5:22–9.
[10] Crostack HZ, Oppermann W. Determination of the optimum centre frequency for ultrasonic testing of sound-scattering materials. Ultrasonics 1983;21(1):19–26.
[11] Sanjie J, Bilgutay NM. Quantitative grain size evaluation using ultrasonic backscattered echoes. J Acoust Soc Am 1986;80:1816–24.
[12] Round WH, Bates RHT. Modification of spectra of pulses from ultrasonic transducers by scatters in non-attenuating and in attenuating media. Ultrason Imaging 1987;9:18–28.
[13] Stephen WF, Norbert JP, Gary HG, Frank DG, Maurice ML. Spectral characterization and attenuation measurements in ultrasound. Ultrason Imaging 1983;5:95–116.
[14] Zhao B, Basir OA, Mittal GS. Estimation of ultrasound attenuation and dispersion using short time Fourier transform. Ultrasonics 2005;43:375–81.
[15] Izquierdo MAG, Hernandez MG, Anaya JJ. Time-varying prediction filter for structural noise reduction in ultrasonic NDE. Ultrasonics 2006;44:1001–5.
[16] Drai Redouane, Khelil Mohamed, Benchaala Amar. Time frequency and wavelet transform applied to selected problems in ultrasonics NDE. NDT&E Int 2002;35:567–72.
[17] Lai WL, Kind T, Wiggenhauser H. Using ground penetrating radar and time–frequency analysis to characterize construction materials. NDT&E Int 2011;44:111–20.
[18] Pachori Ram Bilas, Sircar Pradip. A new technique to reduce cross terms in theWigner distribution. Digital Signal Process 2007;17:466–74.
[19] Cohen L. Time–frequency distributions—A review. Proc. IEEE 1989;77:941–81.
[20] Tang Baoping, Liu Wenyi, Song Tao. Wind turbine fault diagnosis based on Morlet wavelet transformation and Wigner–Ville distribution. Renewable Energy 2010;35:2862–6.
[21] Qian S, Chen D. Joint time–frequency analysis, methods and applications. Prentice Hall 1996; Englewood Cliffs, NJ, USA.
[22] Mannan SL. Influence of grain size on the flow and fracture in AISI type 316 stainless steel at elevated temperatures, PhD thesis, IISc Bangalore, India; 1981.
[23] ASTM standard E 112-96; Standard test methods for determining average grain size; 2004.
[24] Bergner P, Popp K. Mechanisms of ultrasonic attenuation in a bainitic low-alloy steel. Scripta Metall Mater 1990;24:1357.
[25] Papadakis EP. In: Mason WP, Thurston RN, editors. Physical acoustics, vol. XI. New York: Academic; 1975. p. 152–211.
[26] Papadakis EP. Revised grain scattering formulas and tables. J Acoust Soc Am 1965;37:703–10.
[27] Honjoh Katsuhiko. Evaluation techniques for austenitic stainless steels through tensile deformation by analyzing ultrasonic pulses in the frequency domain. Jpn J Appl Phys 1994;33:1554–60.
[28] Jayakumar T. Microstructural characterization in metallic materials using ultrasonic and magnetic methods, PhD thesis, University of Saarland, Saarbruecken, Germany; 1997.